Original Article

Artesunate alleviates myocardial ischemia/reperfusion-induced myocardial necrosis in rats and hypoxia/reoxygenation-induced apoptosis in H9C2 cells via regulating the FAK/PI3K/Akt pathway

Shunyang Fan[1#], Deyin Zhang[2#], Fuyun Liu[3], Yuqi Yang[1], Hongliang Xu[1]

[1]Department of Heart Center, [2]Department of Galactphore, [3]Department of Pediatric Orthopaedic, The Third Affiliated Hospital of Zhengzhou University, Zhengzhou, China

Contributions: (I) Conception and design: S Fan, D Zhang; (II) Administrative support: F Liu; (III) Provision of study materials or patients: S Fan, D Zhang, Y Yang, H Xu; (IV) Collection and assembly of data: S Fan, D Zhang, Y Yang, H Xu; (V) Data analysis and interpretation: S Fan, D Zhang, Y Yang, H Xu; (VI) Manuscript writing: All authors; (VII) Final approval of manuscript: All authors.

[#]These authors contributed equally to this work.

Correspondence to: Fuyun Liu. Department of Pediatric Orthopaedic, The Third Affiliated Hospital of Zhengzhou University, Zhengzhou, China. Email: fuyunliuzzdx3@sina.com.

Background: The various anti-inflammatory, anti-apoptotic, and antioxidant effects of Artesunate (Art) have been explored in numerous studies. This study aimed to evaluate the function of Art on myocardial necrosis in apoptotic cardiomyocytes *in vivo* and *in vitro*.

Methods: Sprague Dawley (SD) rats were randomly divided into groups: a control group, a myocardial ischemia reperfusion (MI/R) group, and MI/R+ Art groups. To establish a MI/R model, rats were subjected to left anterior descending artery ischemia for 45 minutes, and then reperfusion for 2 hours. Hypoxia was induced in H9C2 cells by subjecting them to hypoxic conditions at 37 ℃ for 4 hours, before placing them in a normoxic chamber for 2 hours. The test methods were used in this test, such as echocardiography, enzyme-linked immunosorbent assay (ELISA), HE staining, TUNEL staining, immunohistochemistry, flow cytometry, western blot, and CCK-8 assay.

Results: Art improved myocardial systolic function caused by MI/R injury *in vivo*. Simultaneously, Art reduced the levels of cardiac troponin I (cTnl), creatine kinase-MB (CK-MB) and myohemoglobin (Mb) *in vivo* and *in vitro*. Moreover, Art inhibited cardiomyocyte apoptosis *in vivo* and *in vitro*. The focal adhesion kinase (FAK)/phosphatidylinositide-3 kinases (PI3K)/AKT signaling pathway was also activated by Art *in vivo* and *in vitro*. Furthermore, after inhibitor PF573228 was added, Art inhibited apoptosis in H9C2 cells via activation of the FAK/PI3K/AKT signaling pathway *in vitro*.

Conclusions: This study confirms that Art alleviated MI/R injury and inhibited cardiomyocyte apoptosis *in vivo* and *in vitro*. Art exerted an inhibitory effect on cardiomyocyte apoptosis by activating the FAK/PI3K/AKT signaling pathway. Therefore, Art may serve as an alternative treatment for MI/R injury.

Keywords: Artesunate; myocardial ischemia/reperfusion; hypoxia/reoxygenation; apoptosis; focal adhesion kinase/phosphatidylinositide-3 kinases/Akt pathway (FAK/PI3K/Akt pathway)

Submitted Jun 04, 2020. Accepted for publication Aug 25, 2020.
doi: 10.21037/atm-20-5182
View this article at: http://dx.doi.org/10.21037/atm-20-5182

Introduction

Myocardial ischemia-reperfusion (MI/R) injury is a myocardial injury caused by ischemia and the restoration of blood flow. MI/RI can aggravate myocardial damage and in some cases permanently injures the heart (1,2). The main pathological mechanisms of MI/RI are the massive release of free oxygen radicals, intracellular pH changes, loss of intracellular and mitochondrial calcium homeostasis, reticulum stress, promotion of apoptosis, immune imbalance, myocardial energy metabolism disorders, and myocardial microvascular endothelial cell damage (3,4). Apoptosis is a well-known participant in the pathological process of MI/RI (5).

Artesunate (Art), a sesquiterpene lactone derivative of the Chinese plant Artemisia annua (6). Art has been shown to alleviate bovine serum albumin-induced hepatic fibrosis through matrix metalloproteinase regulation in rats (7). In rheumatoid arthritis rats, Art was observed to suppress chondrocyte proliferation and promote apoptosis and autophagy via PI3K/AKT/mTOR signaling pathway inhibition (8). In a study by Qin *et al.*, Art induced reactive oxygen species (ROS)-independent apoptosis through the Bax-mediated intrinsic pathway in HepG2 cells (9). Furthermore, Art attenuates hemorrhagic shock-related organ injury/dysfunction by activating the mechanism of Akt-endothelial nitric oxide synthase survival as well as inhibiting the mechanism of glycogen synthase kinase-3β and nuclear factor kappaB (10). Interestingly, Khan *et al.* reported for the first time that applying of Art at the beginning of reperfusion can reduce I/R-associated myocardial injury. At the same time, Art is related to the activation of the PI3K/Akt/ERK 1/2 (RISK) and STAT3 (SAFE) pathways, as well as the activation of endothelial nitric oxide synthase (11).

Focal adhesion kinase (FAK), a non-receptor tyrosine kinase, makes a crucial contribution to focal adhesion (FA) assembly by accelerating cytoskeleton dynamics and regulating cell motility (12). Caffeoylserotonin inhibits THP-1 monocyte migration and adhesion via suppressing the integrin β1/FAK/Akt signalling pathway (13). After traumatic brain injury in rats, milk fat globule-EGF factor-8 (MFG-E8) inhibits neuronal apoptosis and offers neuroprotection via the regulation of integrin-β3/FAK/PI3K/AKT signaling (14). Following renal I/R injury, FAK initiates stress response in cells mediated by c-Jun N-terminal kinase, which suggests it may be a potential target for protecting against renal injury (15). Importantly, previous research has demonstrated that enhanced cardiac FAK activity can improve I/R-induced cardiomyocyte apoptosis by activating the surviving NF-κB signaling pathway (16).

At present, whether artemisinin plays a protective role in myocardial ischemia-reperfusion injury has not been reported. Here, we explored the role of Art on MI/R and hypoxia/reoxygenation (H/I) induced cardiomyocyte apoptosis, and further evaluated the function Art on FAK/PI3K/Akt pathway. Our experimental data confirmed that Art alleviates MI/R-induced myocardial necrosis in rats and H/I-induced apoptosis in H9C2 cells via regulating the FAK/PI3K/Akt pathway.

We present the following article in accordance with the ARRIVE reporting checklist (available at http://dx.doi.org/10.21037/atm-20-5182).

Methods

MI/R model and Art-treatment

The animal experiments were conducted in line with the National Institute of Health's Guidelines for the Care and Use of Laboratory Animals and received approval from the Third Affiliated Hospital of Zhengzhou University. Six-to-eight-week-old Sprague Dawley (SD) specific-pathogen-free (SPF) rats (Female, weight: 250–280 g) were divided randomly into five groups: the control group; the MI/R group; the 37.5 mg/kg Art group; the 70 mg/kg Art group; and the 150 mg/kg Art group. Each group of rats was kept in pathogen-free conditions under a 12 h light/12 h darkness cycle at 25±3 ℃ and a relative humidity of 60%. The MI/R model was surgically induced as previously described (17). Rats underwent left anterior descending artery ischemia for 45 minutes, followed by reperfusion for 2 hours. The same surgery was performed on the sham-operated animals, with the exception of the suture being passed under the left anterior descending artery but without ligation.

Art (#A3731) acquired from Sigma-Aldrich (St. Louis, MO, USA) was intraperitoneally injected every day (37.5, 70, 150 mg/kg) for 7 days. On day 3, 24 h after the MI/R model was built successfully, Creatine kinase-MB (CK-MB) and cTnI markers were measured by taking blood samples from the tail vein of the rats.

Echocardiography

Echocardiography was performed as previously described (18). The heart rate (HR), left ventricular end

systolic volume (LVESV), and left ventricular wall thickness (LVWT) of the rats were detected. Left ventricular ejection fraction (LVEF%) = [Left ventricular end-diastolic dimension (LVEDV) – LVESV]/LVEDV × 100%.

Histology

Sodium pentobarbital (40–60 mg/kg) was intraperitoneally injected to anesthetize the rats and the heart tissue was subsequently removed. Hematoxylin and eosin staining (H&E staining) was carried out to histologically assess heart injury using a light microscope. Briefly, heart tissues from the rats were fixed in 4% paraformaldehyde. After 24 hours, the tissues were embedded in paraffin, and cut into 4-μm-thick sections. H&E staining was performed, and a light microscope was used to observe histopathological morphology.

Determination of myocardial enzymes, oxides index and cytokines

Samples of arterial blood collected from the rats were added to heparinized centrifuge tubes. The supernatant was collected and stored at –80 ℃. Enzyme-linked immunosorbent assay kits (ELISA) (Jiancheng, Nanjing, China) were used to measure myocardial enzymes cTnl, CK-MB, and Mbin accordance with the protocol of the manufacturer.

Western blotting

Total protein was extracted from the rat heart tissues and H9C2 cells with 1 mL ice-cold RIPA buffer containing 2 mM phenylmethylsulfonyl fluoride (PMSF) and cocktail. Protein concentration was determined with a BCA kit (Beyotime Institute of Biotechnology, Shanghai, China). The total protein sample (quantity: 20 μg/μL) was loaded into 10% sodium dodecyl sulfate-polyacrylamide gel electrophoresis (SDS PAGE) loading buffer and subsequently transferred to polyvinylidene difluoride (PVDF) membranes. The PVDF membranes were sealed with 5% skim milk at 37 ℃ for 120 min and then incubated with the following primary antibodies: rabbit β-actin (1:1,000, #4970, Cell Signaling), rabbit anti-cleaved caspase-3 (1:1,000, #9661, Cell Signaling), rabbit anti-Bax (1:1,000, #5023, Cell Signaling), rabbit anti-Bcl-2 (1:1,000, #3498, Cell Signaling) at 4 ℃ overnight. After that, the membranes were incubated with goat anti-rabbit IgG horseradish peroxidase (HRP)-conjugated secondary antibodies. Enhanced horseradish peroxidase (Pierce, Rockford, IL, USA) was employed to visualize the signals. The density of the bands was determined and analyzed using an automatic digital gel image analysis system, Bio-Rad CFX-96 (Bio-Rad, CA, USA). β-actin served as the control.

Flow cytometry analysis

The tissue and cell suspension were transferred to a 15 mL centrifuge tube. After 5 minutes of centrifugation, PBS buffer was added to resuspend the tissue and cells. The apoptosis rate was detected using an Annexin V-FITC/propidium iodide (PI) apoptosis detection kit (Multisciences, Shanghai, China). After washing with ice-cold PBS for three times, cells were resuspended and incubated with 5 μL of Annexin V-FIFC and 10 μL of PI. A flow cytometer (BD Biosciences, NY, USA) was used to analyze cell apoptosis. The data were analyzed with FlowJo (Tree Star, OR, USA).

Immunohistochemistry and TUNEL staining

The rat heart tissues were fixed with 4% paraformaldehyde. After 24 hours, the tissues were embedded in paraffin and cut into sections. Xylene was used to separate the paraffinized sections before they were rehydrated using gradient ethanol. Then, antigen extraction was carried out with 10 mM citric acid buffer, and the tissue sections were incubated in 3% H_2O_2 for 10 minutes and sealed at room temperature for 1 hour. Subsequently, the sections were subjected to overnight incubation with rabbit anti-caspase-3 antibody (1:1,000, #9662, Cell Signaling). The corresponding second antibody was incubated at room temperature for 1 hour. Terminal deoxynucleotidyl transferase-mediated dUTP-biotin nick end labeling (TUNEL) staining was carried out to measure cell apoptosis *in situ* in accordance with the instructions of the manufacturer (TUNEL Apoptosis detection kit: UPSTATE, Lake Placid, NY, USA). Apoptotic cells were defined as those with nuclei stained yellowish-brown. Images were captured with a special OLYMPUS DX51 fluorescence microscope (Tokyo, Japan). The data were analyzed by image 6.0.

H9C2 cell culture and H/R injury

As described previously, H9C2 cardiomyocytes were

cultured in Dulbecco's Modified Eagle's Medium (DMEM) (Gibco Laboratories) supplemented with 10% fetal bovine serum (FBS) (Gibco Laboratories) and 1% penicillin/streptomycin in an atmosphere of 90% air and 10% CO_2 at 37 ℃ (19). The experiment was performed with the control, H/R, low-dose (2.5 μM Art), medium-dose (5 μM Art), and high-dose (10 μM Art) groups. To explore the effect of the Art and FAK pathway inhibitor PF573228 on H/R injury, another experiment was performed with the control, H/R, H/R + PF573228 group, the H/R + PF573228 + Art (10 μM Art) group. Inhibitors that do not affect the morphology or viability of H9C2 cells were used. Hypoxia was established by culturing H9C2 cells for 4 hours at a constant temperature three-gas incubator with a mixture of 95% N_2, 5% CO_2, and 1% O_2 at 37 ℃. After that, the cells were reoxygenated in a normoxic chamber for 2 hours. A myocardial cell model (H9C2 cells) of hypoxia/reoxygenation (H/R) was established.

The FAK inhibitor PF573228 was obtained from Sigma-Aldrich (St. Louis, MO) and dissolved with dimethyl sulfoxide (DMSO) to a final concentration of <0.1% per assay.

Cell viability assay

A CCK-8 Assay Kit (Jiancheng, Nanjing, China) was used to determine cell viability. Cells were cultured in a 96-well plate at a density of 1×10^4 cells/well and incubated for 24 to 48 hours. Art was added at final concentrations of 0.3125, 0.625, 1.25, 2.5, 5, 10, 20, 40, 80, and 100 μM. A Perkin Elmer Microplate Reader (PerkinElmer Victor 1420, USA) was used to detect absorbance (at 450 nm).

Statistical analysis

All experimental data were presented as the mean ± standard deviation (SD). SPSS Statistical analyses were performed using SPSS 22.0 software (SPSS Inc., Chicago, IL, USA). Comparisons between two groups were carried out using Student's *t*-test. Differences between the groups were compared by one-way analysis of variance (ANOVA), and Duncan's method was used as a post-hoc test. Each experiment was performed independently at least in triplicate.

Results

Effect of Art on cardiac injury in the MI/R rat model

As shown in *Figure 1A,B,C,D*, the results of echocardiography showed that HR, LVWT, and LVEF were reduced in the MI/R group in comparison with the control group, whereas LVESV was increased. However, after Art treatment, the HR, LVWT, and LVEF were significantly increased compared with the MI/R group, while LVESV was decreased. Moreover, *Figure 1E,F,G* shows that the expression levels of cTnl, CK-MB, and Mb were obviously up-regulated in the MI/R group in comparison with the control group. However, after Art treatment, the levels of cTnl, CK-MB, and Mb were down-regulated in comparison with the H/R group. These results indicated that Art could alleviate myocardial injury in MI/R model.

Effect of Art on myocardial apoptosis in the MI/R model

As shown in *Figure 2*, H&E staining of heart tissue from the MI/R rats displayed that the cardiomyocytes were disordered, the cells were swollen, and some cells were dissolved. TUNEL staining and flow cytometry showed that myocardial apoptotic cells were increased in the MI/R group compared with the control group. Further, immunohistochemical staining showed that the protein expressive levels of caspase-3 were enhanced in cardiac tissue in comparison with the control group. The results of western blot showed an elevated ratio of Bax/Bcl-2. However, after Art treatment, TUNEL staining and flow cytometry showed that myocardial apoptotic rates were decreased in the Art treatment group compared with the MI/R group. Additionally, immunohistochemical staining showed suppressed protein expressive levels of caspase-3 in cardiac tissue compared with the MI/R group. The results of western blot showed that the ratio of Bax/Bcl-2 was restrained. These findings indicated that Art had an inhibitive effect on myocardial apoptosis in the MI/R model.

Effect of Art on FAK/PI3K/Akt pathway in the MI/R model

As *Figure 3* shows, the protein expressive levels of p-FAK, p-P13K, and p-AKT were significantly down-regulated in the MI/R group compared with the control group. However, the protein expressive levels of p-FAK, p-P13K, and p-AKT were significantly up-regulated in the Art treatment group compared with the MI/R group. This indicated that Art activated the FAK/PI3K/Akt pathway in the MI/R model.

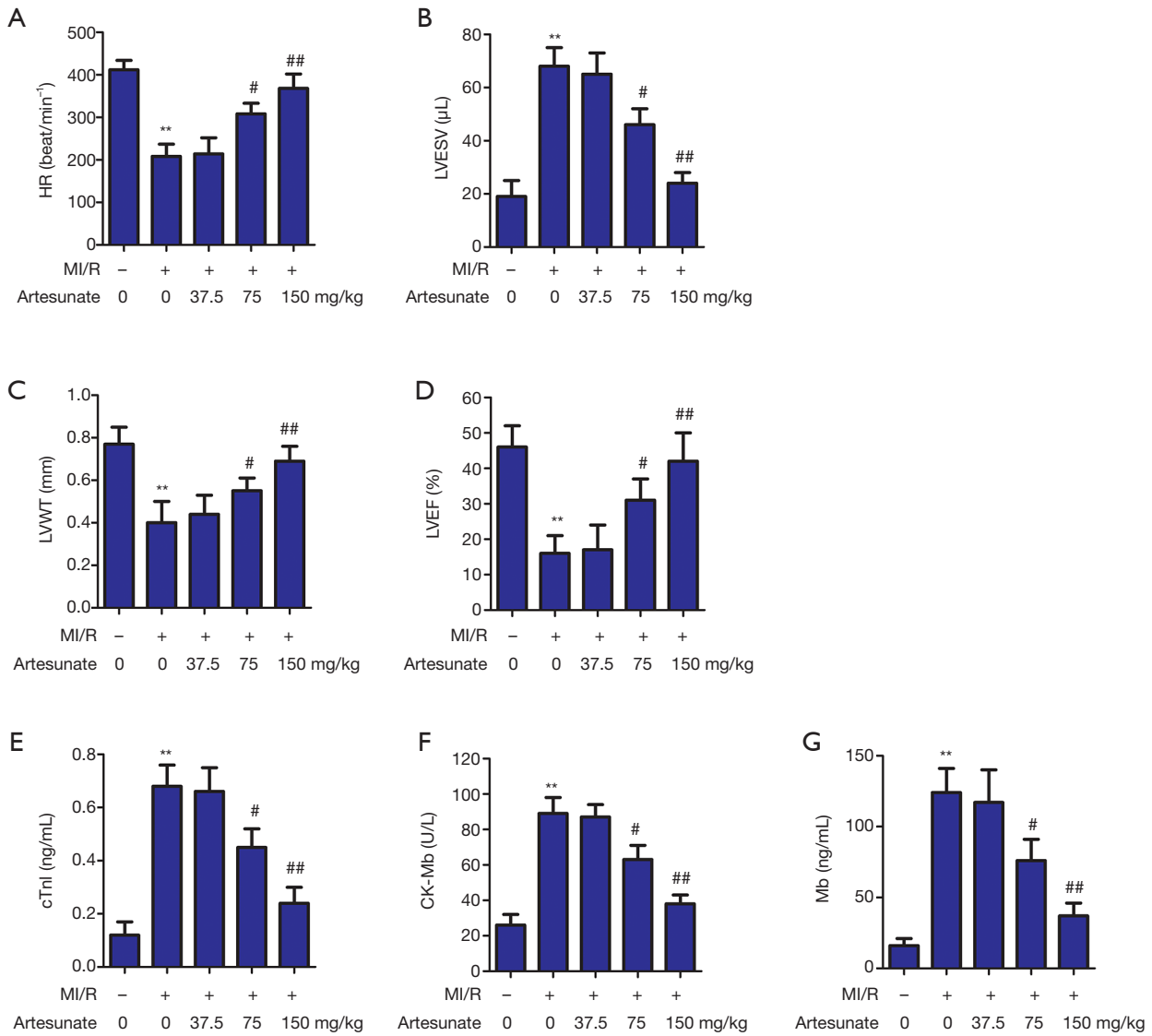

Figure 1 Effect of Art on cardiac injury in the MI/R model. Rats were randomly divided into 5 groups: the control group; the MI/R group; the 37.5 mg/kg Art group; the 70 mg/kg Art group; and the 150 mg/kg Art group. (A) HR (beat/min), (B) LVESV (μL), (C) LVWT (mm), and (D) LVEF (%) were detected by echocardiography. An enzyme-linked immunosorbent assay (ELISA) was carried out to measure the levels of (E) cTnI, (F) CK-MB, and (G) Mb. **, P<0.05 *vs.* the control group; #, P<0.05 *vs.* the MI/R group; ##, P<0.01 *vs.* the MI/R group. MI/R, myocardial ischemia reperfusion; HR, heart rate; LVESV, left ventricular end systolic volume; LVWT, left ventricular wall thickness; LVEF, left ventricular ejection fraction; cTnI, cardiac troponin I; CK-MB, creatine kinase-MB; Mb, myohemoglobin.

Effect of Art on H9C2 cell apoptosis in the H/R model

As shown in *Figure 4A*, the results of the cell viability assay showed that concentrations of 2.5, 5, and 10 μM should be selected for the subsequent experiments. As *Figure 4B,C,D* shows, the expression levels of cTnI, CK-MB, and Mb were clearly up-regulated in the H/R group in comparison with the control group. However, after Art treatment, the levels of cTnI, CK-MB, and Mb were down-regulated compared with the H/R model. Flow cytometry revealed that the apoptotic rate of H9C2 cells was increased in comparison with the control group after Art treatment. However, the apoptotic rate of H9C2 cells was reduced in comparison with the H/R group after Art treatment (*Figure 4E,F*).

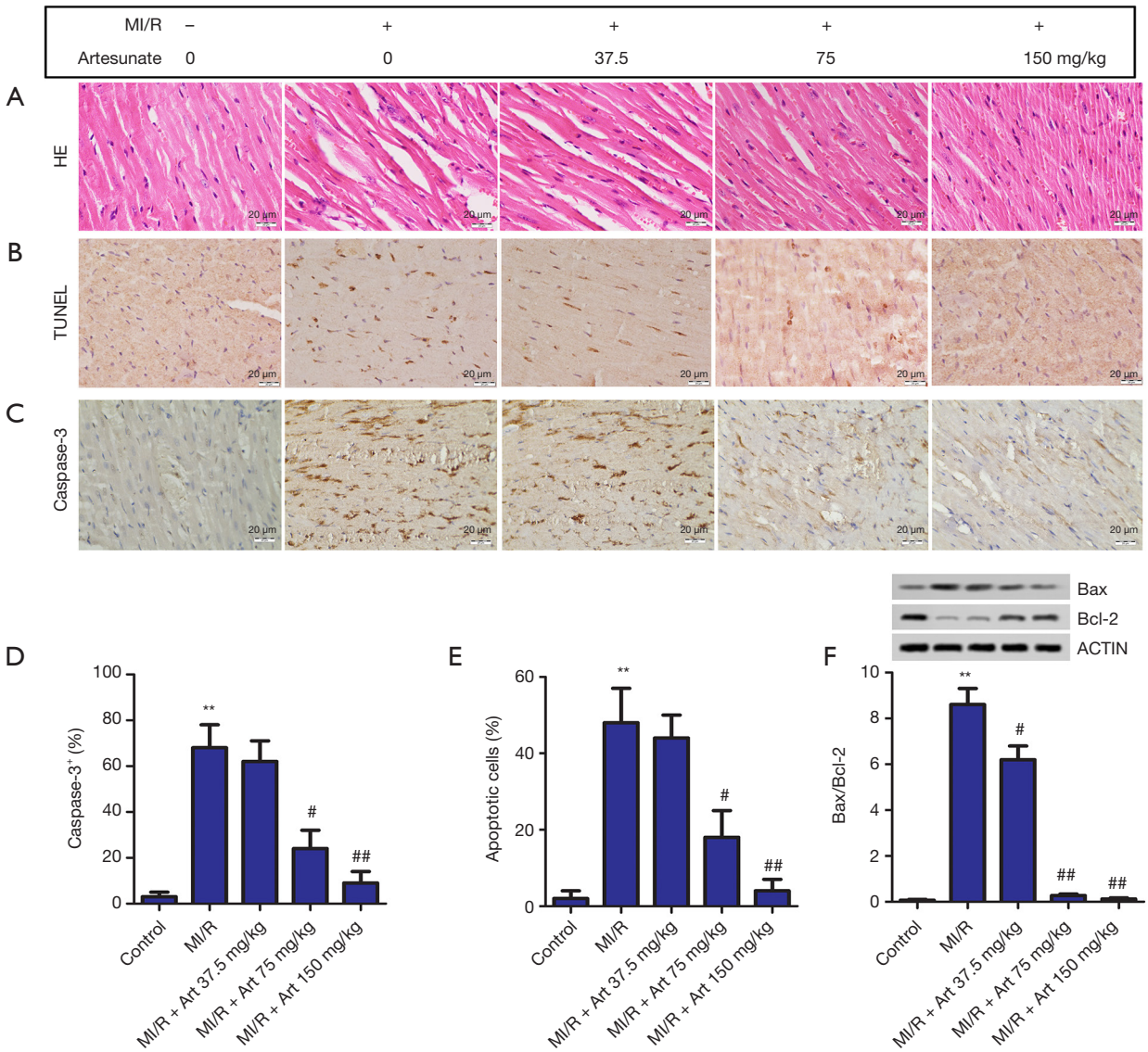

Figure 2 Effect of Art on myocardial apoptosis in the MI/R model. (A) H&E staining of heart tissues from the in MI/R rats revealed that the cardiomyocytes were disordered, the cells were swollen, and some cells were dissolved. Magnification 200×; (B) the apoptotic cells were measured by terminal deoxynucleotidyl transferase-mediated dUTP-biotin nick end labeling (TUNEL) staining. Magnification 200×; (C) the expression levels of caspase-3 were detected by immunohistochemical staining. Magnification 200×; (D) the relative level of caspase-3 was analyzed by image 6.0; (E) the relative level of cell apoptosis was analyzed by image 6.0; (F) the protein expression levels of Bax and Bcl-2 were detected by western blot. **, P<0.05 *vs.* the control group; #, P<0.05 *vs.* the MI/R group; ##, P<0.01 *vs.* the MI/R group. MI/R, myocardial ischemia reperfusion.

Furthermore, the protein levels of cleaved caspase-3 and the Bax/Bcl-2 ratio were both higher in the H/R group than in the control group. After treatment with Art, the protein levels of cleaved caspase-3 and the Bax/Bcl-2 ratio were lower in the Art treatment group than in the H/R group (*Figure 4G,H*). These results suggested that Art suppressed H9C2 cell apoptosis in the H/R model.

Effect of Art on FAK/PI3K/Akt pathway in H/R model

As *Figure 5A* shows, the protein expressive levels of p-FAK, p-P13K and p-AKT were inhibited in comparison with the

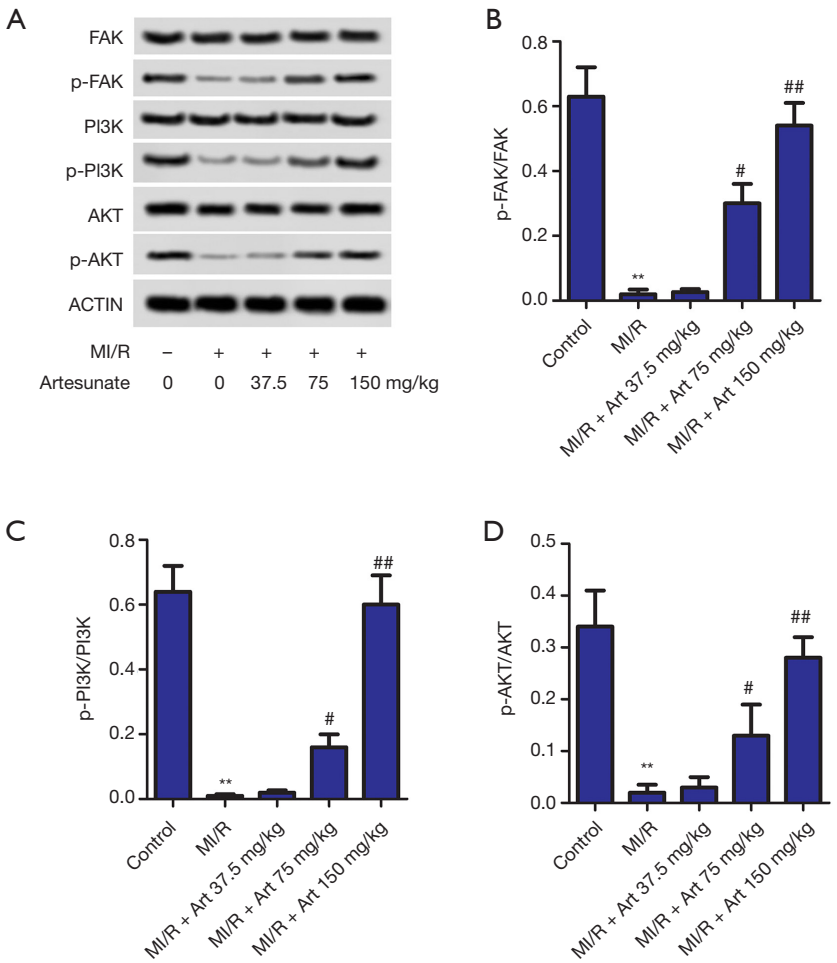

Figure 3 Effect of Art on the FAK/PI3K/Akt pathway in the MI/R model. (A) The protein expression levels of p-FAK, p-P13K, and p-AKT were detected by western blot. Semi-quantitative analysis of the relative levels of p-FAK (B), p-P13K (C), and p-AKT (D) in each group of rats. **, P<0.05 *vs.* the control group; #, P<0.05 *vs.* the MI/R group; ##, P<0.01 *vs.* the MI/R group. MI/R, myocardial ischemia reperfusion.

control group. However, the protein expressive levels of p-FAK, p-P13K, and p-AKT were elevated compared with the H/R group. Subsequently, to verify if Art could activate the FAK/PI3K/Akt pathway, the inhibitor PF573228 was chosen to suppress the FAK/PI3K/Akt pathway. After the addition of PF573228 (*Figure 5B,C,D*), the expressions of cTnl, CK-MB, and Mb were clearly up-regulated in the PF573228 group compared with the H/R group. The rate of cell apoptosis and the Bax/Bcl-2 ratio were both strikingly increased compared with the H/R group. Interestingly, after treatment with PF573228 and Art, the expressions of cTnl, CK-MB, and Mb were clearly down-regulated in the H/R + PF573228 + Art group in comparison with the PF573228 group. The rate of cell apoptosis and the Bax/Bcl-2 ratio were markedly decreased compared with the H/R + PF573228 + Art group (*Figure 5E*).

Discussion

For patients with cardiovascular disease, there are various interventions, such as thrombolytic therapy and coronary artery bypass grafting. However, for MI/R injury, these treatments are not effective. Therefore, further research on the treatment of MI/R injury is needed. At present, The treatment of MI/R injury with traditional Chinese medicine is a popular research area, and a considerable number of studies have shown that traditional Chinese medicine has an important role to play (20,21).

The present study found that Art significantly reduced the levels of cTnl, CK-MB, and Mb in our MI/R model.

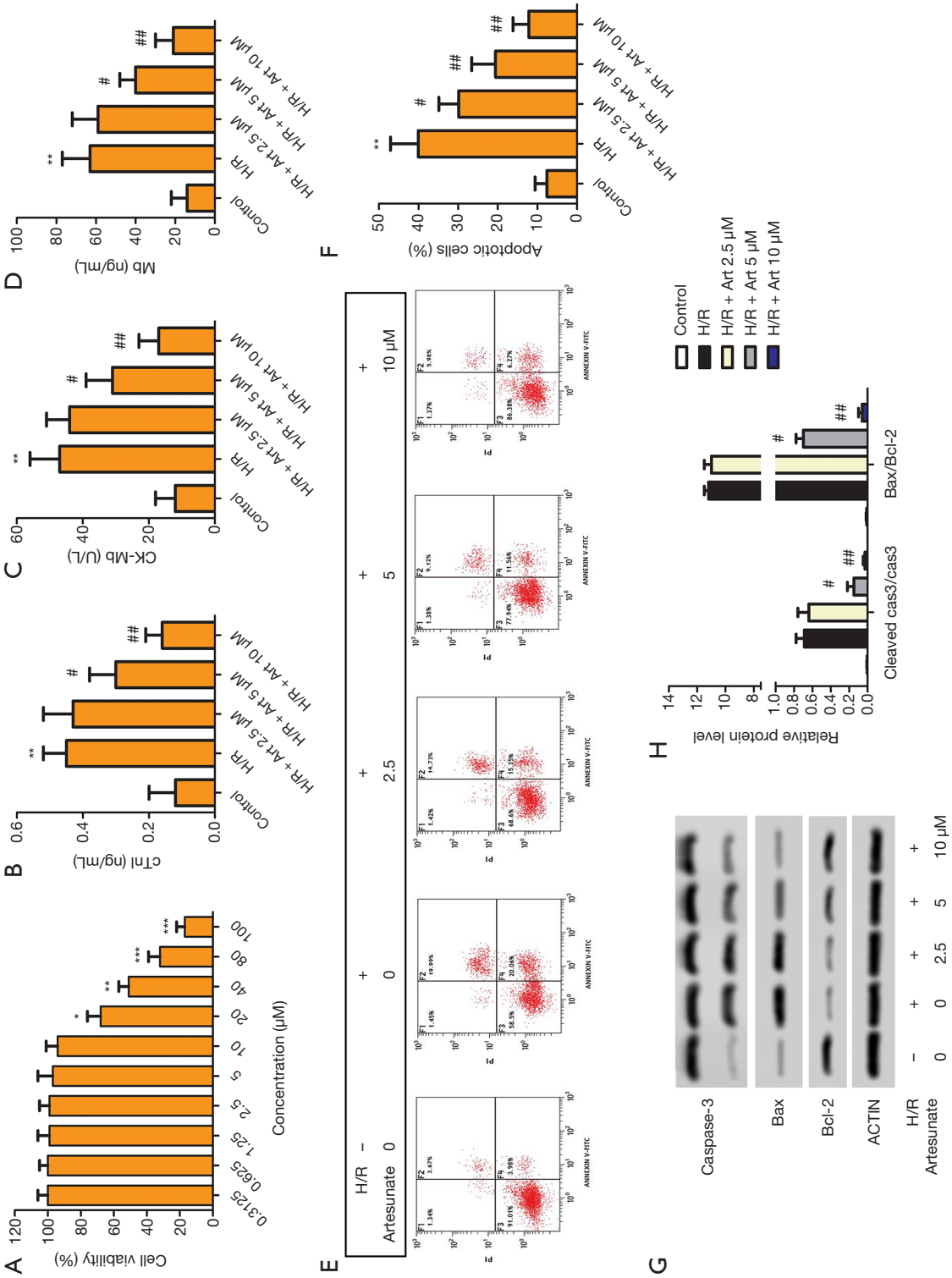

Figure 4 Effect of Art on H9C2 cell apoptosis in the H/R model. (A) Cell viability was detected by CCK-8 assay. H9C2 cells were divided into 5 groups: the control group; the H/R group; the low-dose group (2.5 μM Art); the medium-dose group (5 μM Art); and the high-dose group (10 μM Art). (B) cTnI, (C) CK-MB and (D) Mb were measured by ELISA. (E,F) Cell apoptosis was detected by flow cytometry. The representative column diagrams showing results of number of F2 + F4 as apoptotic cells. (G) The protein expression levels of cleaved caspase-3, Bax, and Bcl-2 were detected by western blot. (H) Semi-quantitative analysis of the relative levels. *, P<0.05 *vs.* the control group; **, P<0.01 *vs.* the control group; ***, P<0.001 *vs.* the control group; #, P<0.05 *vs.* the H/R group; ##, P<0.01 *vs.* the H/R group.

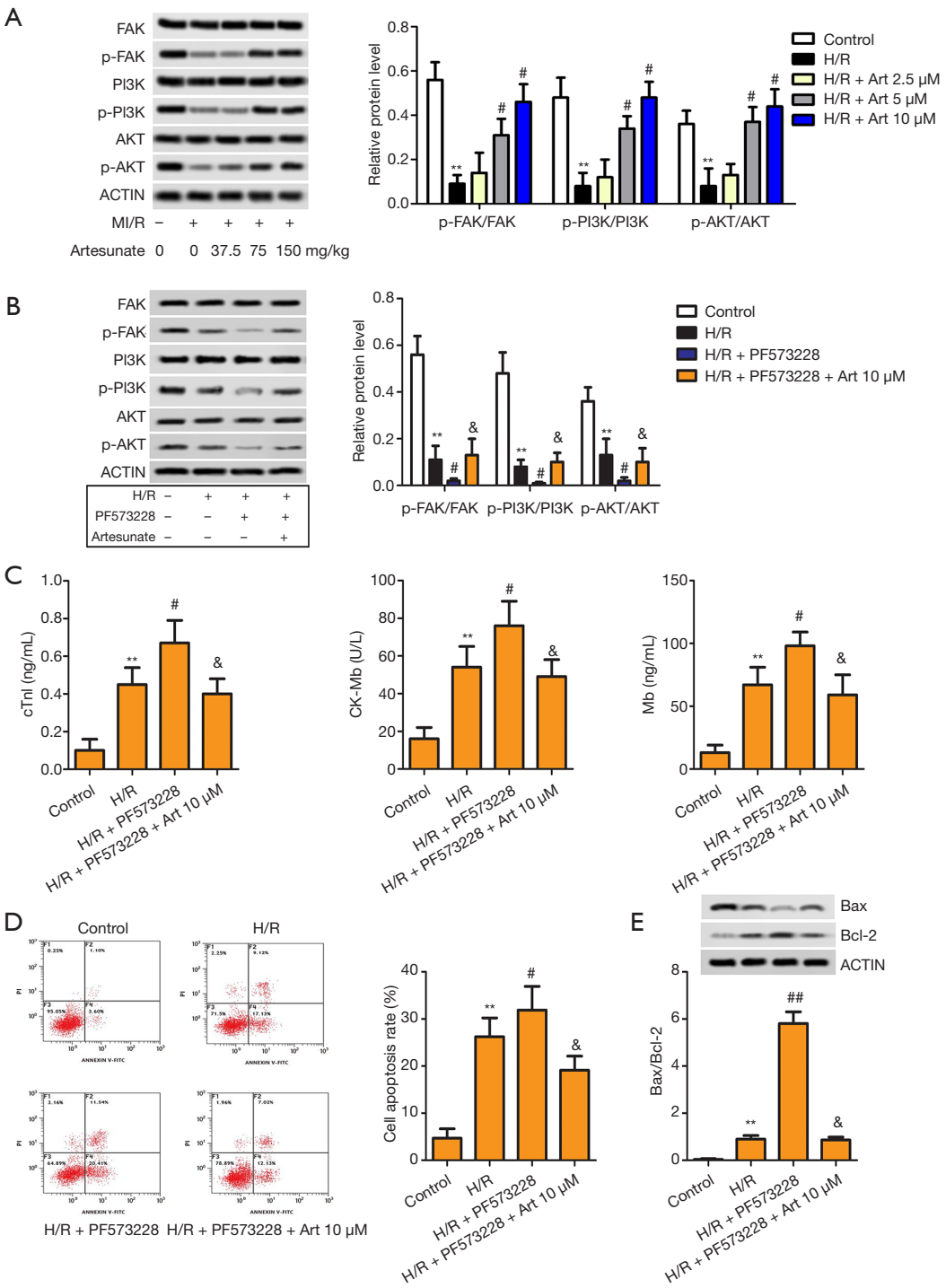

Figure 5 Effect of Art on the FAK/PI3K/Akt pathway in the H/R model. (A) The protein expression levels of p-FAK, p-P13K, and p-AKT were detected by western blot. H9C2 cells were divided into 4 groups: the control group; the H/R group; H/R + PF573228 group; and the H/R + PF573228 + Art group. (B) The protein expression levels of p-FAK, p-P13K, and p-AKT were detected by western blot. (C) ELISA was carried out to measure cTnI, CK-MB, and Mb. (D) Cell apoptosis was detected by flow cytometry. The representative column diagrams showing results of number of F2 + F4 as apoptotic cells. (E) The protein expression levels of Bax and Bcl-2 were detected by western blot. **, P<0.05 *vs.* the control group; #, P<0.05 *vs.* the H/R group; &, P<0.05 *vs.* the H/R + PF573228 group.

Treatment with Art was also shown to improve HR, LVWT, and LVEF, and reduce LVESV. Cui *et al.* found that phosphatase and tensin homolog (PTEN) mRNA and protein levels were significantly reduced, the pathological damage of cardiomyocytes was alleviated, and HR, LVSP, LVEF, FS, and LVWT were significantly elevated in their MI/R model (22). The same study also found that the serum levels of CK-MB, Mb, and cTnI were significantly inhibited. Therefore, these results indicate that Art could improve cardiac contractile function in MI/R rats.

Apoptosis is a well-known participator in the pathological process of MI/R injury (5). MI/R injury induces a sterile inflammatory response, resulting in further injury and an eventual increase in infarct size. The locally released risk-related molecular pattern initiates and triggers the NOD-like receptor protein 3 inflammasome, and enhances the inflammatory response and cell death through activating caspase-1 (23). Many studies have shown that inhibition of the inflammatory response can reduce cardiomyocyte apoptosis in the pathological process of myocardial I/R injury (24). Our study found that Art treatment suppressed myocardial apoptosis.

Previous research has exhibited that a downstream molecule of the integrin receptor FAK, suppresses apoptosis by activating the downstream effector Akt (25,26). FAK alleviates radiation-induced rectal injury by decreasing apoptosis (27). Interestingly, FAK activation may facilitate tumour initiation by causing resistance to apoptosis (28). Simulated-microgravity reduces focal adhesions (FAs) and alters the cytoskeleton and nuclear positioning, leading to enhance cell apoptosis via suppressing the FAK/RhoA-regulated mTORC1/NF-κB and ERK1/2 pathways (29). Long non-coding RNAs (lncRNAs) MIR22HG abrogation inhibits proliferation and induces apoptosis in esophageal adenocarcinoma cells via activation of the STAT3/c-Myc/FAK signaling (30). Song *et al.* reported that the expression levels of tissue inhibitor matrix metalloproteinase 1 (TIMP1) were inhibited by the activation of TIMP1 specific regulated FAK-PI3K/AKT and MAPK pathway (31). Art regulates the proliferation, apoptosis, and activation of LX-2 cells. Moreover, Art's anti-fibrogenic mechanism is related to the FAK/Akt/β-catenin pathway (32). Importantly, a previous study noted that enhancement of cardiac FAK activity via activation of the prosurvival NF-κB pathway can attenuate I/R-induced cardiomyocyte apoptosis (16). Our study found that Art treatment led to the suppressed expression of caspase-3 and Bax as well as the up-regulation of Bcl-2 expression *in vivo* and *in vitro* via regulation of the FAK/PI3K/AKT signaling pathway. Despite the levels of the proapoptotic protein Bcl-2 being up-regulated, the levels of the antiapoptotic proteins Bax and caspase-3 were high enough to inhibit the apoptosis induced by Bcl-2 in myocardial cells. These results suggest that Art inhibits cardiomyocyte apoptosis *in vivo* and *in vitro*.

PF573228 is widely used as an inhibitor of the FAK signaling pathway (33,34). In PF573228-treated cells, the levels of p-FAK, p-P13K, and p-AKT were reduced, while the expression levels of cTnl, CK-MB, and Mb were clearly up-regulated. The rate of cell apoptosis was markedly increased along with the Bax/Bcl-2 ratio. However, the expression levels of cTnl, CK-MB, and Mb were observably down-regulated in the H/R + PF573228 + Art group. The cell apoptosis rate and Bax/Bcl-2 ratio were markedly reduced compared with those in the H/R + PF573228 + Art group. These results prove that Art inhibits the cardiomyocyte apoptosis signaling pathway *in vitro*.

Conclusions

Art improved myocardial systolic function caused by MI/R injury *in vivo*. Art also reduced the levels of myocardial enzymes cTnl, CK-MB, and Mb, and inhibited cardiomyocyte apoptosis *in vivo* and *in vitro*. Furthermore, Art activated the FAK/PI3K/AKT signaling pathway *in vivo* and *in vitro*. After the addition of FAK inhibitor PF573228, Art inhibited apoptosis of H9C2 cells via activating the FAK/PI3K/AKT signaling pathway *in vitro*. This study confirms that Art treatment was able to alleviate MI/R injury and inhibit cardiomyocyte apoptosis *in vivo* and *in vitro*. Art's inhibitory effect on cardiomyocyte apoptosis was regulated through activation of the FAK/PI3K/AKT signaling pathway. Therefore, Art may provide an alternative treatment for MI/R injury.

Acknowledgments

Funding: This study was supported by the Scientific Research Project of Henan Provincial Science and Technology Department (182102310433) and Henan Medical Science and Technology Public Relations Project (2018020203).

Footnote

Reporting Checklist: The authors have completed the ARRIVE reporting checklist. Available at http://dx.doi.

org/10.21037/atm-20-5182

Data Sharing Statement: Available at http://dx.doi.org/10.21037/atm-20-5182

Conflicts of Interest: All authors have completed the ICMJE uniform disclosure form (available at http://dx.doi.org/10.21037/atm-20-5182). The authors have no conflicts of interest to declare.

Ethical Statement: The authors are accountable for all aspects of the work in ensuring that questions related to the accuracy or integrity of any part of the work are appropriately investigated and resolved. The animal experiments were conducted in line with the National Institute of Health's Guidelines for the Care and Use of Laboratory Animals and received approval from the Third Affiliated Hospital of Zhengzhou University.

References

1. Hausenloy DJ, Yellon DM. Myocardial ischemia-reperfusion injury: a neglected therapeutic target. J Clin Invest 2013;123:92-100.
2. Hou X, Fu M, Cheng B, et al. Galanthamine improves myocardial ischemia-reperfusion-induced cardiac dysfunction, endoplasmic reticulum stress-related apoptosis, and myocardial fibrosis by suppressing AMPK/Nrf2 pathway in rats. Ann Transl Med 2019;7:634.
3. Vincent A, Covinhes A, Barrère C, et al. Acute and long-term cardioprotective effects of the Traditional Chinese Medicine MLC901 against myocardial ischemia-reperfusion injury in mice. Sci Rep 2017;7:14701.
4. Braunersreuther V, Jaquet V. Reactive oxygen species in myocardial reperfusion injury: from physiopathology to therapeutic approaches. Curr Pharm Biotechnol 2012;13:97-114.
5. Guo CX, Jiang X, Zeng XJ, et al. Soluble receptor for advanced glycation end-products protects against ischemia/reperfusion-induced myocardial apoptosis via regulating the ubiquitin proteasome system. Free Radic Biol Med 2016;94:17-26.
6. Kong Z, Liu R, Cheng Y. Artesunate alleviates liver fibrosis by regulating ferroptosis signaling pathway. Biomed Pharmacother 2019;109:2043-53.
7. Xu Y, Liu W, Fang B, et al. Artesunate ameliorates hepatic fibrosis induced by bovine serum albumin in rats through regulating matrix metalloproteinases. Eur J Pharmacol 2014;744:1-9.
8. Feng FB, Qiu HY. Effects of Artesunate on chondrocyte proliferation, apoptosis and autophagy through the PI3K/AKT/mTOR signaling pathway in rat models with rheumatoid arthritis. Biomed Pharmacother 2018;102:1209-20.
9. Qin G, Wu L, Liu H, et al. Artesunate induces apoptosis via a ROS-independent and Bax-mediated intrinsic pathway in HepG2 cells. Exp Cell Res 2015;336:308-17.
10. Sordi R, Nandra KK, Chiazza F, et al. Artesunate Protects Against the Organ Injury and Dysfunction Induced by Severe Hemorrhage and Resuscitation. Ann Surg 2017;265:408-17.
11. Khan AI, Kapoor A, Chen J, et al. The Antimalarial Drug Artesunate Attenuates Cardiac Injury in A Rodent Model of Myocardial Infarction. Shock 2018;49:675-81.
12. Al-Ghabkari A, Qasrawi DO, Alshehri M, et al. Focal adhesion kinase (FAK) phosphorylation is a key regulator of embryonal rhabdomyosarcoma (ERMS) cell viability and migration. J Cancer Res Clin Oncol 2019;145:1461-9.
13. Yoon JH, Kim HE, Choi JY, et al. Caffeoylserotonin suppresses THP-1 monocyte adhesion and migration via inhibition of the integrin β1/FAK/Akt signalling pathway. Fitoterapia 2012;83:1364-70.
14. Gao YY, Zhang ZH, Zhuang Z, et al. Recombinant milk fat globule-EGF factor-8 reduces apoptosis via integrin β3/FAK/PI3K/AKT signaling pathway in rats after traumatic brain injury. Cell Death Dis 2018;9:845.
15. Qin Y, Alderliesten MC, Stokman G, et al. Focal adhesion kinase signaling mediates acute renal injury induced by ischemia/reperfusion. Am J Pathol 2011;179:2766-78.
16. Cheng Z, DiMichele LA, Hakim ZS, et al. Targeted focal adhesion kinase activation in cardiomyocytes protects the heart from ischemia/reperfusion injury. Arterioscler Thromb Vasc Biol 2012;32:924-33.
17. Yan X, Anzai A, Katsumata Y, et al. Temporal dynamics of cardiac immune cell accumulation following acute myocardial infarction. J Mol Cell Cardiol 2013;62:24-35.

18. Zhang Q, Deng Y, Lai W, et al. Maternal inflammation activated ROS-p38 MAPK predisposes offspring to heart damages caused by isoproterenol via augmenting ROS generation. Sci Rep 2016;6:30146.
19. Qiu Z, Lei S, Zhao B, et al. NLRP3 Inflammasome Activation-Mediated Pyroptosis Aggravates Myocardial Ischemia/Reperfusion Injury in Diabetic Rats. Oxid Med Cell Longev 2017;2017:9743280.
20. Liu K, Chen H, You QS, et al. Curcumin attenuates myocardial ischemia-reperfusion injury. Oncotarget 2017;8:112051-9.
21. Ye B, Chen X, Dai S, et al. Emodin alleviates myocardial ischemia/reperfusion injury by inhibiting gasdermin D-mediated pyroptosis in cardiomyocytes. Drug Des Devel Ther 2019;13:975-90.
22. Cui Q, Wang J, Liu X, et al. Knockout of PTEN improves cardiac function and inhibits NLRP3-mediated cardiomyocyte pyroptosis in rats with myocardial ischemia-reperfusion. Xi Bao Yu Fen Zi Mian Yi Xue Za Zhi 2020;36:205-11.
23. Toldo S, Mauro AG, Cutter Z, et al. Inflammasome, pyroptosis, and cytokines in myocardial ischemia-reperfusion injury. Am J Physiol Heart Circ Physiol 2018;315:H1553-68.
24. Feng L, Liu W, Yang J, et al. Effect of Hexadecyl Azelaoyl Phosphatidylcholine on Cardiomyocyte Apoptosis in Myocardial Ischemia-Reperfusion Injury: A Hypothesis. Med Sci Monit 2018;24:2661-7.
25. Farrelly N, Lee YJ, Oliver J, et al. Extracellular matrix regulates apoptosis in mammary epithelium through a control on insulin signaling. J Cell Biol 1999;144:1337-48.
26. Matter ML, Ruoslahti E. A signaling pathway from the alpha5beta1 and alpha(v)beta3 integrins that elevates bcl-2 transcription. J Biol Chem 2001;276:27757-63.
27. Li JJ, Tu WZ, Chen XM, et al. FAK alleviates radiation-induced rectal injury by decreasing apoptosis. Toxicol Appl Pharmacol 2018;360:131-40.
28. Walker S, Foster F, Wood A, et al. Oncogenic activation of FAK drives apoptosis suppression in a 3D-culture model of breast cancer initiation. Oncotarget 2016;7:70336-52.
29. Zhao T, Li R, Tan X, et al. Simulated Microgravity Reduces Focal Adhesions and Alters Cytoskeleton and Nuclear Positioning Leading to Enhanced Apoptosis via Suppressing FAK/RhoA-Mediated mTORC1/NF-κB and ERK1/2 Pathways. Int J Mol Sci 2018;19:1994.
30. Su W, Guo C, Wang L, et al. LncRNA MIR22HG abrogation inhibits proliferation and induces apoptosis in esophageal adenocarcinoma cells via activation of the STAT3/c-Myc/FAK signaling. Aging (Albany NY) 2019;11:4587-96.
31. Song G, Xu S, Zhang H, et al. TIMP1 is a prognostic marker for the progression and metastasis of colon cancer through FAK-PI3K/AKT and MAPK pathway. J Exp Clin Cancer Res 2016;35:148.
32. Lv J, Bai R, Wang L, et al. Artesunate may inhibit liver fibrosis via the FAK/Akt/β-catenin pathway in LX-2 cells. BMC Pharmacol Toxicol 2018;19:64.
33. Onofre TS, Rodrigues JPF, Yoshida N. Depletion of Host Cell Focal Adhesion Kinase Increases the Susceptibility to Invasion by Trypanosoma cruzi Metacyclic Forms. Front Cell Infect Microbiol 2019;9:231.
34. Sun X, Meng L, Qiao W, et al. Vascular endothelial growth factor A/Vascular endothelial growth factor receptor 2 axis promotes human dental pulp stem cell migration via the FAK/PI3K/Akt and p38 MAPK signalling pathways. Int Endod J 2019;52:1691-703.

(English Language Editor: J. Reynolds)

Cite this article as: Fan S, Zhang D, Liu F, Yang Y, Xu H. Artesunate alleviates myocardial ischemia/reperfusion-induced myocardial necrosis in rats and hypoxia/reoxygenation-induced apoptosis in H9C2 cells via regulating the FAK/PI3K/Akt pathway. Ann Transl Med 2020;8(20):1291. doi: 10.21037/atm-20-5182

